Hydrol. Earth Syst. Sci. Discuss., 11, 7977–8011, 2014
www.hydrol-earth-syst-sci-discuss.net/11/7977/2014/
doi:10.5194/hessd-11-7977-2014

Hydrology and Earth System Sciences
Discussions
Open Access

Uncertainty propagation in a cascade modelling approach to flood mapping

J. P. Rodríguez-Rincón, A. Pedrozo-Acuña, and J. A. Breña Naranjo

National Autonomous University of México, Institute of Engineering, D.F., Mexico City, Mexico

Received: 7 June 2014 – Accepted: 30 June 2014 – Published: 14 July 2014

Correspondence to: A. Pedrozo-Acuña (apedrozoa@ii.unam.mx)

Published by Copernicus Publications on behalf of the European Geosciences Union.

Abstract

The purpose of this investigation is to study the propagation of meteorological uncertainty within a cascade modelling approach to flood mapping. The methodology is comprised of a Numerical Weather Prediction Model (NWP), a distributed rainfall–runoff model and a standard 2-D hydrodynamic model. The cascade of models is used to reproduce an extreme flood event that took place in the Southeast of Mexico, during November 2009. The event is selected as high quality field data (e.g. rain gauges; discharge) and satellite imagery are available. Uncertainty in the meteorological model (Weather Research and Forecasting model) is evaluated through the use of a multi-physics ensemble technique, which considers twelve parameterization schemes to determine a given precipitation. The resulting precipitation fields are used as input in a distributed hydrological model, enabling the determination of different hydrographs associated to this event. Lastly, by means of a standard 2-D hydrodynamic model, hydrographs are used as forcing conditions to study the propagation of the meteorological uncertainty to an estimated flooded area. Results show the utility of the selected modelling approach to investigate error propagation within a cascade of models. Moreover, the error associated to the determination of the runoff, is showed to be lower than that obtained in the precipitation estimation suggesting that uncertainty do not necessarily increase within a model cascade.

1 Introduction

Despite the lack of a definitive consensus on the possible contribution of climate change to the recent amplification of extreme hydro-meteorological events and the consequent flooding, it has been largely recognised that such hazards are likely to increase given current climate change scenarios (Milly et al., 2007). Indeed, flooding is one of the most common and destructive natural hazards faced by civilization, and recent catastrophes observed worldwide, highlight the need for better flood management strategies.

In September 2013, severe floods were registered in Mexico as a result of the exceptional simultaneous incidence of two tropical storms, culminating in serious damage and widespread persistent flooding (Pedrozo-Acuña et al., 2014a). More recently, in 2014, record-breaking precipitation and flooding was observed in the UK (Slingo et al., 2014). In both cases, the immediate action of governments through the implementation of emergency and action plans was required. The main aim of these interventions was to reduce the duration and impact of floods. In both events, risk reduction measures were designed to ensure both a better flood management and an increase in infrastructure resilience.

One key piece of information in preventing and reducing losses is given by reliable flood inundation maps that enable the dissemination of flood risk to the society and decision makers (Pedrozo-Acuña et al., 2012). Traditionally, this task requires the estimation of different return periods for discharge (Ward et al., 2011) and their propagation to the floodplain by means of a hydrodynamic model. There is currently a large range of models that can be used to develop flood hazard maps (Horrit and Bates, 2002; Horrit et al., 2006).

On the other hand, the accelerated progress of computers and the availability of climate models with sufficient resolution to capture meteorological events and their associated rainfall, has given way to the development of model cascades o produce hydrological forecasts (Bartholomes and Todini, 2005; Demerrit et al., 2010) and flood hazard maps (Cuo et al., 2011; Pappenberger et al., 2012; Pedrozo-Acuña et al., 2013). Within this approach, the coupling of different operational numerical models is carried out, using for example, numerical weather prediction (NWP) with radar data for hydrologic forecast (Liguori and Rico-Ramirez, 2012; Liguori et al., 2012), or NWP with hydrological and hydrodynamic models (Pappenberger et al., 2012; Cloke et al., 2013; Ushiyama et al., 2014).

HESSD
11, 7977–8011, 2014

The use of regional climate models (RCMs) in climate impact studies on flooding has been reported by Teutschbein and Seibert (2010) and Beven (2011), noting that despite their usefulness, the spatial resolution of models (∼ 25 km) remains coarse to capture the spatial resolution of precipitation. This is particularly important as higher resolution is needed to effectively model the hydrological processes essential for determining flood risk. To overcome this limitation, the utilisation of dynamic downscaling in these models is also growing (Fowler et al., 2007; Leung and Qian, 2009; Lo et al., 2008).

Significant challenges remain in the foreseeable future, among these, the inherent uncertainties in the predictive models is likely to have an important role to play. For example, it is well known that the performance skill of NWPs deteriorates very rapidly with time (Lo et al., 2008). To overcome this, the long-term continuous integration of the prediction has been subdivided into short-simulations, involving the re-initialisation of the model to mitigate the problem of systematic error growth in long integrations (Giorgi, 1990, 2006; Qian et al., 2003). Moreover, the use of ensemble prediction systems to obtain rainfall predictions for hydrological forecasts at the catchment scale, is becoming more common among the hydrological community as they enable the evaluation and quantification of uncertainties (Buizza, 2008; Cloke and Pappenberger, 2009; Bartholmes et al., 2009).

A key question that arises when using a cascade modelling approach to flood forecasting or mapping is: how uncertainties associated to meteorological predictions of precipitation propagate to a given flood inundation map? In order to answer this question, the purpose of this investigation is to study the propagation of epistemic uncertainties from the meteorological model to a given flood map. For this, we utilize a cascade modelling approach comprised by a Numerical Weather Prediction Model (NWP), a rainfall–runoff model and a standard 2-D hydrodynamic model. The numerical framework is applied to an observed extreme event registered in Mexico in 2009. Uncertainty is considered in the NWP model using a multi-physics ensemble technique considering several multi-physics parameterization schemes for the precipitation (Bukosvky and Karoly, 2009). The resulting precipitation fields are used to generate spaghetti plots by

HESSD
11, 7977–8011, 2014

means of a distributed hydrological model, enabling the propagation of meteorological uncertainties to the runoff. Hence, the resulting hydrographs represent the runoff associated to each precipitation field estimated with the NWP. In order to complete the propagation of the uncertainty though the cascade of models to the flood map, the hydrographs are used as forcing in a standard 2-D hydrodynamic model.

On the other hand, it is acknowledged that each of the other models (hydrological and hydrodynamic) within the model cascade, will introduce epistemic and random uncertainties to the result. In order to reduce their influence, the numerical setup of both these models is constructed with the best available data (e.g. LiDAR for the topography) and following recent guidelines for the assessment of uncertainty in flood risk mapping (Beven et al., 2011). In this way, the uncertainty associated to the meteorological model outputs is propagated through the model cascade from the atmosphere to the flood map. Thus, the aim of this investigation is to study the propagation of epistemic errors within the first stage of the model cascade, to the determination of an affected area impacted by a well-documented hydro-meteorological event.

This work is organised as follows: Sect. 2 provides a description of both, the study area and the extreme hydro-meteorological event, which are employed to test our cascade modelling approach; Sect. 3 introduces the methodology, incorporating a brief description of the selected models setup. Additionally, we incorporate a description of the multi-physics ensemble technique used to quantify and limit the epistemic uncertainty in the NWP model. The resulting precipitation fields, hydrographs and flood maps are compared with available field data and satellite imagery for the event. In Sect. 4, a discussion of errors along the model cascade, is also presented with some conclusions and future work.

2 Case study

The selected study area is within the Mexican state of Tabasco, which in recent years has been subjected to severe flooding as reported by Pedrozo-Acuña et al. (2011, 2012). This region comprises the area of Mexico with the highest precipitation rate (2000–3000 mm year^{-1}), which mostly occurs during the wet season of the year between May and December. The rainfall climatology is also influenced by the incidence of hurricanes and tropical storms arriving from the North.

In this paper, the extreme hydro-meteorological event selected for the analysis corresponds to that registered in the early days of November 2009 in the Tonalá river. As it is shown in Fig. 1, the river is located in the border of Tabasco and Veracruz and during the event, the substantial rainfall intensity provoked its overflowing leaving extensive inundated areas along its floodplain. Top panel of Fig. 1 shows the geographical location of the catchment, with an area of 5021 km^2, as well as the location of 18 weather stations installed within the region by the National Weather Service. The event was the result of heavy rain induced by the cold front #9, which persisted for four days along Mexico's Gulf Coast, forcing more than 44 000 people to evacuate their homes and affecting more than 90 communities. High intensities in rainfall were recorded in rain gauges from the 31 October to 3 November, with cumulative daily precipitation values reporting more than 270 mm. The river is approximately 300 km long and before discharging into the Gulf of Mexico, the stream receives additional streamflow from other smaller streams such as Agua Dulcita in Veracruz, and Chicozapote in Tabasco. The bottom panel of the same Figure illustrates the lower Tonalá River, where severe flooding was registered as it is shown in the photographs on the right. The yellow, blue and red dots on the panel represent the location at which the photographs were taken.

The hydrometric data in combination with the satellite imagery for the characterisation of the affected areas, enabled an accurate investigation of the causes and consequences that generated this flood event. The high quality of the available information, allowed the application of a cascade modelling approach comprised by state-of-the-art meteorological, hydrological and hydrodynamic models. This numerical approach is utilised with the intention to carry out an assessment of the modelling framework, with particular emphasis on the propagation of the epistemic uncertainty from the meteorological model to the spatial extent of an affected area. Such investigation paves the

HESSD
11, 7977–8011, 2014

road towards a more honest knowledge transfer to decision-makers, whom consider the reliability of the model results.

3 Methodology and results

The methodology is comprised of a Numerical Weather Prediction Model (NWP), a distributed rainfall–runoff model and a standard 2-D hydrodynamic model. It is anticipated that the selected modelling approach will support the advance of the understanding of the connections among scales, intensities, causative factors, and impacts of extremes. This model cascade with state-of-the-art numerical tools representing a hydrological system, enables the development of a framework by which an identification of the reliability of simulations can be undertaken. This framework is utilised to explore the propagation of epistemic uncertainties from the estimation of precipitation in the atmosphere to the identification of a flooded area. Therefore, the aim is not to reproduce an observed extreme event, but to investigate the effects of errors in rainfall prediction by a NWP on inundation areas.

The proposed investigation is important as uncertainties are cascaded through the modelling framework, in order to provide better understanding on how errors propagate within models working at different temporal and spatial scales. It is acknowledged that this information would enhance better flood management strategies, which would be based on the honest and transparent communication of the results produced by a modelling system constrained by intrinsic errors and uncertainties.

3.1 Meteorological model

Simulated precipitation products from numerical weather prediction systems (NWPs) typically show differences in their spatial and temporal distribution. These differences can considerably influence the ability to predict hydrological responses. In this sense, in this study we utilise the advanced research core of the Weather Research and

HESSD
11, 7977–8011, 2014

Forecasting (WRF) model Version 3.2. The WRF model is a fully compressible non-hydrostatic, primitive-equation model with multiple nesting capabilities (Skamarock et al., 2008).

As it is shown in Fig. 2, the model setup is defined using an interactive nested domain inside the parent domain. This domain is selected in order to simulate more realistic rainfall, with the inner frame enclosing the Tonalá river catchment within a 4 km resolution. The 4 km horizontal resolution is considered good enough to compute a mesoscale cloud system associated to a cold front. It is shown that this finer grid covers the central region of Mexico, while in the vertical dimension, 28 unevenly spaced sigma levels were selected. The initial and boundary conditions were created from the NCEP Global Final Analysis (FNL) with a time interval of 6 h for the initial and boundary conditions. Each of the model simulations was reinitialised every two days at 12:00 UTC, considering a total simulation time from 27 October 2009 until 13 November 2009.

Epistemic uncertainty is considered in the WRF model by means of the sensitivity of the results for precipitation, due to variations in the model setup. For this, we utilise a multi-physics ensemble technique proposed by Bukovsky and Karoly (2009), where the sensitivity of simulated precipitation in the model results is examined with twelve different parameterisation schemes. The comparison of computed precipitation fields against real measurements from weather stations within the catchment, enabled the quantification of uncertainty in the meteorological model for this event. Table 1 shows a summary of the different multi-physics parameters used in the WRF model to generate the physics ensemble. In this approach, the multi-physics ensemble runs of the model represent a plausible and equally likely state of the system in the future.

Figure 3 illustrates the cumulative precipitation fields computed for each of the 12 selected members of the multi-physics ensemble, where differences in the spatial distribution and intensity of precipitation were evident. These results suggested that for this event, the precipitation field estimated with the WRF was highly sensitive to the selection of multi-physics parameters. To revise in more detail the performance of the WRF

HESSD
11, 7977–8011, 2014

in reproducing this hydro-meteorological event, the estimated cumulative precipitation by each member of the multi-physics ensemble was compared against measurements at the eighteen weather stations located within and close to the Tonalá catchment.

Table 2 presents a summary of the most well-known error metrics calculated at each weather station and for each member of the ensemble. Among these are the: Normalised Root-Mean Square Error (NRMSE), BIAS, Nash–Sutcliffe Coefficient (NSC), and the Correlation coefficient (Cor). The columns show the local value of each coefficient for a given member of the ensemble (M1, ..., M12). As shown in all columns (i.e. member runs), the error metrics have a great spatial variability, hence, indicating the regions of the study area where the model performs better. To illustrate the performance of this ensemble technique at each weather station, the ensemble average of these error metrics are introduced in the last column and indicated by $\langle\,\rangle$. Again, the spatial variability of the metrics is evident. The two bottom rows in each sub-table correspond to the average of the ensemble averages for the whole catchment and for the all the stations. It is shown, that when the average of all stations is taken into account, the skill decreases. However, in this investigation the error that is of interest is the one corresponding to the average of those weather stations located within the catchment, as these will be used as input in the hydrological model. This will enable the propagation of errors in the meteorological model within the model cascade. For clarity, in the same table the stations within the catchment are highlighted in blue.

Additionally, results per station are also illustrated for four different cases and are presented in Fig. 4, and they confirmed that the range of spatial uncertainty in the WRF predictions is high and variable. To give an example, at Station No. 27075, the spread of the estimated cumulative precipitation curves is limited and quantified by a NSC = 0.917 and a NRMSE = 10.7 %, indicating a good skill of the WRF precipitation estimates at this point. In contrast, at Station No. 27007 the spread of the cumulative precipitation is large and characterised by a NSC = 0.766 and a NRMSE = 19.4 %, showing less skill in the model performance than that observed in the previous case. The observed differences of estimated precipitation for this event, highlight the

HESSD
11, 7977–8011, 2014

importance of incorporating ensemble techniques in the reproduction of precipitation with this type of models.

A question that has been seldom explored in the literature, is how the uncertainty in the prediction of the precipitation (i.e. errors described in this section), cascade into an estimated flood hydrograph determined by a distributed hydrological model. In this sense, the next step in this work, considers the non-linear transfer of rainfall to runoff using a distributed rainfall–runoff model. For this, we employ each one of the 12 precipitation fields derived from the WRF as input to determine the associated river discharge with the hydrological model.

3.2 Hydrological model

The hydrological model used in this study was applied to the Tonalá River catchment in an early work presented by Rodríguez-Rincón et al. (2012). This numerical tool was developed by the Institute of Engineering – UNAM (Domínguez-Mora et al., 2008), and comprises a simplified grid-based distributed rainfall–runoff model. The model has been previously applied with success in other catchments in Mexico (e.g. Pedrozo-Acuña et al., 2014b).

This paper only describes an overview and key components of the hydrologic model. Interested readers can find detailed descriptions in Domínguez-Mora et al. (2008). The model is based on the method of the Soil Conservation Service (SCS) with a modification that allows the consideration of soil moisture accounting before and after rainfall events. The parameters that are needed for the definition of a runoff curve number within the catchment are the hydrological soil group, land use, pedology and the river drainage network. Figure 5 shows for the Tonalá River catchment, the spatial definition of the river network (center panels) and runoff curve (right panels). The model is forced with the precipitation calculated from the WRF considering the 12 members of the multi-physics ensemble.

It is well known that both the amount and distribution of rainfall can significantly affect the final estimated river discharge (Ferraris et al., 2002; De Roo et al., 2003; Xuan et al., 2005). In consequence, the propagation of meteorological uncertainty to the rainfall–runoff model is carried out using WRF rainfall precipitation ensembles as an input in the hydrological model. For this purpose, free-parameters in the hydrologic model are fixed, assuming that the selected parameters are the best at representing the physical conditions of the catchment for this event. The selection of these parameters is carried out following the results presented by Rodríguez-Rincón et al. (2012) for the same catchment. For the numerical setup of the hydrological model, we employ topographic information from a LiDAR data set, from which a 10 m resolution Digital Elevation Model (DEM) is constructed.

Figure 6 illustrates for the Tonalá River catchment the spaghetti plot of hydrographs computed for this event, these are shown along with the measured discharge by a streamflow gauge. The uncertainty bounds illustrated by the grey shaded area indicate that errors in the predicted rainfall are indeed propagated to the hydrological model, which uses a finer spatial resolution (1 km). It has been established that, in some cases, an error in the meteorological model can be compensated by an error in the hydrological model and vice-versa. To illustrate this in more detail, Table 3 presents a summary of the error metrics for the hydrographs shown in Fig. 6. It is shown that on average (last column in the Table) the hydrological model has a NSC = 0.84, Cor = 0.96, BIAS = 1.01 and NRMSE = 38.12 %. Differences between members of the multi-physics ensemble are also illustrated at this stage, especially by the NSC. For instance, member M11 indicates a NSC = 0.68 showing poor skill at reproducing the river discharge with the precipitation derived from this member, in contrast member M3 has a greater skill with NSC = 0.93. The change in the values of the NSC indicates that results from the regional weather model can be enhanced or weakened by the performance of the hydrological model.

The use of these hydrographs in a 2-D hydrodynamic model, enables the study of the propagation of errors within the cascade of models. In particular, for estimating the flood extent during this extreme event.

HESSD
11, 7977–8011, 2014

3.3 Flood inundation model

Several 2-D hydrodynamic models have been developed for simulating extreme flood events. However, any model is only as good as the data used to parameterise, calibrate and validate the model. 2-D models have been regarded as suitable for simulating problems where inundation extent changes dynamically through time as they can easily represent moving boundary effects (e.g. Bates and Horritt, 2005). The use of these numerical tools has become common place when flows produce a large areal extent, compared to their depth and where there are large lateral variations in the velocity field (Hunter et al., 2008).

In this study, given the size of the study area the modelling system utilised is comprised by the flow model of MIKE 21 flexible mesh (FM). This numerical model solves the two dimensional Reynolds-averaged Navier–Stokes equations invoking the approximations of Boussinesq and hydrostatic pressure. This involves continuity, momentum, temperature, salinity and density equations (for details see DHI, 2014). The equations are solved at the centre of each element in the model domain.

The numerical setup is based on a previous work on the study area (Pedrozo-Acuña et al., 2012), with selected resolutions for the elements of the mesh with a size that guarantees the proper assimilation of a 10 m DEM to characterise the elevation in the floodplain. The topographic data has been regarded as the most important factor in determining water surface elevations, base flood elevation, and the extent of flooding and, thus, the accuracy of flood maps in riverine areas (NRC, 2009). Therefore, the elevation data used in this study corresponds to LiDAR data provided by INEGI (2008). The hydraulic roughness in the floodplain is assumed to be uniform and different from the main river channel, in this sense two values for the Manning number are used, one for the main river channel ($M = 32\,\mathrm{m}^{1/2}\,\mathrm{s}^{-1}$) and another for the floodplain ($M = 28\,\mathrm{m}^{1/2}\,\mathrm{s}^{-1}$). The choice of a 10 m DEM is based on recommendations put forward by the Committee on Floodplain Mapping Technologies, NRC (2007) and Prinos et al. (2008), as such a DEM ensures both accuracy and detail of the ground surface.

HESSD
11, 7977–8011, 2014

The model domain is illustrated in Fig. 7, along with the numerical mesh and elevation data, it comprises the lower basin of the Tonalá River and additional main water bodies. The colours represent the magnitude of the elevation and bathymetric data assimilated in the numerical mesh, where warm colours identify high ground areas and light blues represent bathymetric data. The numerical mesh considers three boundary conditions represented in the Figure by dots as follows: where the input hydrograph from the rainfall–runoff model is set (red dot); the Tonalá's river mouth, where the astronomical tide for the period of the event (27 October–12 November 2009) (yellow dot) and the Agua Dulcita river set where a constant discharge of 100 $m^3 s^{-1}$ is introduced (blue dot).

It is acknowledged that topographic information is key for the reduction of uncertainty in flood hazard mapping. Therefore, in order to minimise this source of error, the integration of high quality topographic information in a 2-D model with enough spatial resolution, will enable the investigation of the propagation of the meteorological uncertainty to the determination of the flood extent.

Figure 8a introduces the result of the hydrodynamic simulation for each of the 12 hydrographs, which resulted from the utilisation of the rainfall–runoff model using as input the WRF multi-physics ensemble. The illustrated flood map summarises the 12 different possibilities of inundation area that could result from the characterisation of precipitation with the WRF model. Differences in the size of these areas, illustrate the propagation of epistemic errors from the meteorological model to the flood map. In this sense, the analysis of uncertainty has been restricted to its propagation along the model chain (atmosphere-catchment-river floodplain). Each of these flood maps can also be associated to a probability enabling the representation of a probabilistic flood map, shown in the figure. This allows the identification of the areas highly vulnerable to flooding from this event. Additionally, Fig. 8b introduces the infrared SPOT satellite image of the 12 November 2009, which is used for comparison against the produced flood maps using all the ensemble members. Notably, in the numerical results, the blue area identifies the region of the domain that is most likely to be flooded (90 %), the comparison of this area with the observed inundation in the satellite image, show a good skill of the model chain at reproducing the registered flood in the study area.

To better quantify the performance of each of the model runs in reproducing the observed flood extent, the estimation of several error metrics in these results was also performed, among these are: BIAS, False Alarm Ratio (FAR), Probability of Detection (POD), Probability of False Detection (POFD), Critical Success Index (CSI) and the True Skill Statistics (TSS). Table 4 introduces the results by member and metric. Clearly, there is some variability in the performance of the model for each of the ensemble members, showing that there has been some propagation of the error to the flood map. The ensemble average of these quantities is also illustrated in the last column of the table, where a BIAS = 0.964, FAR = 0.453, POD = 0.799, POFD = 0.154; CSI = 0.831 and TSS = 0.645 are reported. These results indicate a good skill of the model chain at reproducing the flood extension, due to the incidence of this extreme event.

Current approaches to flood mapping, have pointed out that in order to produce a scientifically justifiable flood map, the most physically-realistic model should be utilised (Di Baldassarre et al., 2010). Nevertheless, even with these models the amount of uncertainty involved in the determination of an affected area is important and should be quantified.

4 Discussion and conclusions

It has been largely acknowledged in the literature, that flood risk mapping and assessment are highly difficult tasks due to the inherent complexity of the relevant processes, which occur in several spatial and temporal scales. As pointed out by Aronica et al. (2013), the process is subject to substantial uncertainties (epistemic and random), which emerge from different sources and idealisation of processes, from the statistical analysis of extreme events and from the resolution and accuracy of the DEM used in a flood inundation model.

HESSD
11, 7977–8011, 2014

By acknowledging that all models are an imperfect representation of the reality, it is important to quantify the impact of epistemic uncertainties on a given result. The numerical approach utilised in this investigation enabled an assessment of a state-of-the art modelling framework, comprised by meteorological, hydrological and hydrodynamic models. Emphasis was given to the effects of epistemic uncertainty propagation from the meteorological model to the definition of an affected area in a 2-D domain. Ensemble climate simulations have become a common practice in order to provide a metric of the uncertainty associated with climate predictions. In this study, a multi-physics ensemble technique is utilised to evaluate the propagation of epistemic uncertainties within a model chain. Therefore, the assessment of hydro-meteorological model performance at the three stages is carried out through the estimation of skill scores.

Figure 9 presents a summary of the propagation of two well-known error metrics, BIAS (top panel) and NSC/TSS (bottom panel). These metrics are selected, as they enable a direct comparison of their values at each of the stages within the model cascade. In both metrics, the evolution of the confidence limits is illustrated by the size of the bars. Their evolution from the meteorological model to the hydrological model results, show a clear decrease in both cases. This result may point towards an enhancement of meteorological uncertainties in the rainfall–runoff model. However, the skill of the hydrological model is considerably improved from a mean value of 0.65 in the meteorological model, to 0.834. In the last stage of the model chain, the confidence limits of the results at the hydrodynamic model results, show a small improvement. Nevertheless, the mean value of the skill is reduced to TSS = 0.645. The results provide a useful way to evaluate the uncertainty propagation within the whole hydro-meteorological modelling system.

It should be pointed out, that this methodology contains more uncertainties that were not considered or quantified in the generation of flood extent maps for this event. To quantify the epistemic uncertainty in the larger scale (i.e. atmosphere), a mesoscale numerical weather system was used along with a multi-physics ensemble. The ensemble was designed to represent our limited knowledge of the processes generating

HESSD
11, 7977–8011, 2014

precipitation in the meteorological system. The propagation of this uncertainty to a rainfall–runoff model revealed large spatial variations of the model skill across scales and models. It was shown that a large amount of uncertainty exists in the NWP, and this is indeed propagated over the catchment and floodplain scales. Members of the ensemble were shown to differ significantly in terms of cumulative precipitation, its spatial distribution, river discharge and the size of the affected area by the event. Therefore, epistemic uncertainties from each step in the hazard analysis chain accumulate in the final outputs.

The evaluation of the skill in the model cascade shows further potential for improvements of the model system. Consequently, future work is planned to include the remaining uncertainties as adopted by, e.g. Pedrozo-Acuña et al. (2013). Special attention should be paid to the interaction of meteorological uncertainty with that of hydrological origin. The assessment of the error propagation within the model cascade is seen as a good step forward, in the communication of uncertain results to the society. The proposed numerical framework could be utilised as a robust alternative for the characterisation of extreme events in ungauged basins.

The acknowledgment of these uncertainties, by showing their impact on model results, favour preventive action in the production of methodologies that evaluate flood extension with some level of confidence. Therefore, the investigation paves the road towards a more honest knowledge transfer to decision-makers, whom consider the reliability of the model results.

Acknowledgements. The authors thank the financial support from the Institute of Engineering, UNAM, through internal and international grants.

HESSD
11, 7977–8011, 2014

Uncertainty propagation in a cascade modelling approach

J. P. Rodríguez-Rincón et al.

References

Aronica, G. T., Apel, H., Baldassarre, G. D., and Schumann, G. J.-P.: HP – special issue on flood risk and uncertainty, Hydrol. Process., 27, 1291, doi:10.1002/hyp.9812, 2013.

Bartholmes and Todini: Coupling meteorological and hydrological models for flood forecasting, Hydrol. Earth Syst. Sci., 9, 333–346, doi:10.5194/hess-9-333-2005, 2005.

Bartholmes, J. C., Thielen, J., Ramos, M. H., and Gentilini, S.: The european flood alert system EFAS – Part 2: Statistical skill assessment of probabilistic and deterministic operational forecasts, Hydrol. Earth Syst. Sci., 13, 141–153, doi:10.5194/hess-13-141-2009, 2009.

Bates, P. D. and Horritt, M. S.: Modelling wetting and drying processes in hydraulic models, in: Computational Fluid Dynamics: Applications in Environmental Hydraulics, edited by: Bates, P. D., Lane, S. N., and Ferguson, R. I., John Wiley and Sons, Chichester, UK, 2005.

Beven, K. J.: I believe in climate change but how precautionary do we need to be in planning for the future?, Hydrol. Process., 25, 1517–1520, 2011.

Beven, K. J., Leedal, D., McCarthy, S., Lamb, R., Hunter, N., Keef, C., Bates, P., Neal, J., and Wicks, J.: Framework for Assessing Uncertainty in Fluvial Flood Risk Mapping, FRMRC Research Report SWP1.7, http://web.sbe.hw.ac.uk/frmrc/downloads/Framework_for_Assessing_Uncertainty_Fluvial_Flood_Risk_Mapping_WP1_7.pdf (last access: 10 July 2014), 2011.

Buizza, R.: The value of probabilistic prediction, Atmos. Sci. Lett., 9, 36–42, 2008.

Bukovsky, M. S. and Karoly, D. J.: Precipitation simulations using WRF as a nested regional climate model, J. Appl. Meteorol. Clim., 48, 2152–2159, 2009.

Cloke, H. L. and Pappenberger, F.: Evaluating forecasts for extreme events for hydrological applications: an approach for screening unfamiliar performance measures, Meteorol. Appl., 15, 181–197, 2008.

Cloke, H. L. and Pappenberger, F.: Ensemble flood forecasting: a review, J. Hydrol., 375, 613–626, doi:10.1016/j.jhydrol.2009.06.005, 2009.

Cloke, H. L., Wetterhall, F., He, Y., Freer, J. E., and Pappenberger, F.: Modelling climate impact on floods with ensemble climate projections, Q. J. Roy. Meteorol. Soc., 139, 282–297, doi:10.1002/qj.1998, 2013.

Committee on FEMA Flood Maps: Board on Earth Sciences and Resources/Mapping Science Committee, NRC: Mapping the Zone: Improving Flood Map Accuracy, National Academic Press, Washington, D.C., 2009.

Committee on Floodplain Mapping Technologies, NRC: Elevation Data for Floodplain Mapping, National Academic Press, Washington, D.C., 2007.

CONAGUA: Atlas Digital del Agua México 2010, Sistema Nacional de Información del Agua, available at: ftp://ftp.conagua.gob.mx/ (last access: 10 July 2014), 2010.

Cuo, L., Pagano, T. C., and Wang, Q. J.: A review of quantitative precipitation forecasts and their use in short to medium range streamflow forecasting, J. Hydrometeorol., 12, 713–728, doi:10.1175/2011JHM1347.1, 2011.

Demeritt, D., Nobert, S., Cloke, H., and Pappenberger, F.: Challenges in communicating and 5 using ensembles in operational flood forecasting, Meteorol. Appl., 17, 209–222, 2010.

de Roo, A. P. J., Gouweleeuw, B., Thielen, J., Bartholmes, J., Bongioannini-Cerlini, P., Todini, E., Bates, P. D., Horritt, M., Hunter, N., Beven, K. J., Pappenberger, F., Heise, E., Rivin, G., Hils, M., Hollingsworth, A., Holst, B., Kwadijk, J., Reggiani, P., Van Dijk, M., Sattler, K., and Sprokkereef, E.: Development of a European flood forecasting system, Int. J. River Basin Manage., 1, 49–59, 2003.

DHI: MIKE 21 FM Flow model, Scientific Documentation, DHI Group, Horslhome, 2014.

Di Baldassarre, G., Schumann, G., Bates, P. D., Freer, J. E., and Beven, K. J.: Floodplain mapping: a critical discussion of deterministic and probabilistic approaches, Hydrolog. Sci. J., 55, 364–376, doi:10.1080/02626661003683389, 2010.

Domínguez, M. R., Esquivel, G. G., Méndez, A. B., Mendoza, R. A., Arganis, J. M. L., and Carrizosa, E. E.: Manual del Modelo para pronóstico de escurrimiento, Instituto de Ingeniería, Universidad Nacional Autónoma de México, Mexico City, Mexico, 2008.

Ferraris, L., Rudari, R., and Siccardi, F.: The uncertainty in the prediction of flash floods in the Northern Mediterranean environment, J. Hydrometeorol., 3, 714–727, 2002.

Fowler, H. J., Blenkinsop, S., and Tebaldi, C.: Linking climate change modelling to impacts studies: recent advances in downscaling techniques for hydrological modelling, Int. J. Climatol., 27, 1547–1578, 2007a.

Giorgi, F.: Simulation of regional climate using a limited area model nested in a general circulation model, J. Climate, 3, 941–963, 1990.

Giorgi, F.: Regional climate modeling: status and perspectives, J. Phys. IV, 139, 101–118, 2006.

Horritt, M. S. and Bates, P. D.: Evaluation of one-dimensional and two-dimensional models for predicting river flood inundation, J. Hydrol., 268, 87–99, 2002.

HESSD

11, 7977–8011, 2014

Uncertainty propagation in a cascade modelling approach

J. P. Rodríguez-Rincón et al.

Horritt, M. S., Bates, P. D., and Mattinson, M. J.: Effects of mesh resolution and topographic representation in 2D finite volume models of shallow water fluvial flow, J. Hydrol., 329, 306–314, doi:10.1016/j.jhydrol.2006.02.016, 2006.

Hunter, M., Bates, P. D., Neelz, S., Pender, G., Villanueva, I., Wright, N. G., Liang, D., Falconer, A., Lin, B., Waller, S., Crossley, A. J., and Mason, D. C.: Benchmarking 2D hydraulic models for urban flooding, Water Manage., 161, 13–30, 2008.

INEGI: Nube de Puntos LIDAR ajustada al Terreno, Bloque conformado por las cartas 1 : 50,000: E15A75, E15A76, E15A85, E15A86 del Instituto Nacional de Estadística, Geografía e Informática, México, Mexico City, Mexico, 2008.

Jankov, I., Gallus, W. A., Segal, M., Shaw, B., and Koch, S. E.: The impact of different WRF model physical parameterizations and their interactions on warm season MCS rainfall, Weather Forecast., 20, 1048, doi:10.1175/WAF888.1, 2005.

Leung, L. R. and Qian, Y.: Atmospheric rivers induced heavy precipitation and flooding in the western US simulated by the WRF regional climate model, Geophys. Res. Lett., 36, L03820, doi:10.1029/2008GL036445, 2009.

Liguori, S. and Rico-Ramirez, M. A.: Quantitative assessment of short-term rainfall forecasts from radar nowcasts and MM5 forecasts, Hydrol. Process., 26, 3842–3857, 2012.

Liguori, S., Rico-Ramirez, M. A., Schellart, A., and Saul, A.: Using probabilistic radar rainfall nowcasts and NWP forecasts for flow prediction in urban catchments, Atmos. Res., 103, 80–95, 2012.

Lo, J. C. F., Yang, Z. L., and Pielke, Sr., R. A.: Assessment of three dynamical climate downscaling methods using the Weather Research and Forecasting (WRF) model, J. Geophys. Res., 113, D09112, doi:10.1029/2007JD009216, 2008.

Milly, P. C. D., Wetherland, R. T., Dunne, K. A., and Delworth, T. L.: Increasing risk of great floods in a changing climate, Nature, 415, 514–517, doi:10.1038/415514a, 2002.

Pappenberger, F., Beven, K. J., Hunter, N. M., Bates, P. D., Gouweleeuw, B. T., Thielen, J., and de Roo, A. P. J.: Cascading model uncertainty from medium range weather forecasts (10 days) through a rainfall-runoff model to flood inundation predictions within the European Flood Forecasting System (EFFS), Hydrol. Earth Syst. Sci., 9, 381–393, doi:10.5194/hess-9-381-2005, 2005.

Pappenberger, F., Dutra, E., Wetterhall, F., and Cloke, H. L.: Deriving global flood hazard maps of fluvial floods through a physical model cascade, Hydrol. Earth Syst. Sci., 16, 4143–4156, doi:10.5194/hess-16-4143-2012, 2012.

HESSD
11, 7977–8011, 2014

Uncertainty propagation in a cascade modelling approach

J. P. Rodríguez-Rincón et al.

Pedrozo-Acuña, A., Mariño-Tapia, I., Enriquez Ortiz, C., Medellín Mayoral, G., and González-Villareal, F. J.: Evaluation of inundation areas resulting from the diversion of an extreme discharge towards the sea: case study in Tabasco, Mexico, Hydrol. Process., 26, 687–704, 2011.
Pedrozo-Acuña, A., Ruiz de Alegria-Arzaburu, A., Mariño-Tapia, I., Enriquez, C., and González-Villareal, F. J.: Factors controlling flooding at the Tonalá river mouth (Mexico), J. Flood Risk Manage., 5, 226–244, doi:10.1111/j.1753-318X.2012.01142.x, 2012.
Pedrozo-Acuña, A., Rodríguez-Rincón, J. P., Arganis-Juárez, M., Domínguez-Mora, R., and González-Villareal, F. J.: Estimation of probabilistic flood inundation maps for an extreme event: Pánuco River, México, J. Flood Risk Manage., doi:10.1111/jfr3.12067, in press, 2013.
Pedrozo-Acuña, A., Mejía-Estrada, P. I., Rodríguez-Rincón, J. P., Domínguez-Mora, R., and González-Villareal, F. J.: Flood Risk From Extreme Events in Mexico, 11th International Conference on Hydroinformatics, New York, USA, 2014a.
Pedrozo-Acuña, A., Breña-Naranjo, J. A., and Domínguez-Mora, R.: The Hydrological Setting of the 2013 Floods in Mexico, Weather, Wiley and Sons, accepted, 2014b.
Prinos, P., Kortenhaus, A., Swerpel, B., and Jiménez, J. A.: Review of Flood Hazard Mapping, Floodsite Report No. T03-07-01, 54, http://www.floodsite.net/html/partner_area/project_docs/T03_07_01_Review_Hazard_Mapping_V4_3_P01.pdf (last access: 10 July 2014), 2008.
Qian, J.-H., Seth, A., and Zebiak, S.: Reinitialized versus continuous simulations for regional climate downscaling, Mon. Weather Rev., 131, 2857–2874, 2003.
Rodríguez-Rincón, J. P., Pedrozo-Acuña, A., Domínguez Mora, R., Reeve, D. E., and Cluckie, I.: Probabilistic Estimation of Flood Maps: an Ensemble Approach, FloodRisk2012, The 2nd European Conference on FLOODrisk Management, Rotterdam, the Netherlands, 2012.
Skamarock, W. C., Klemp, J. B., Dudhia, J., Gill, D. O., Barker, D. M., Duda, M. G., Huang, X.-Y., Wang, W., and Powers, J. G.: A description of the Advanced Research WRF version3, NCAR Technical Note NCAR/TN475+STR, National Center for Atmospheric Research – NCAR, Boulder, Colorado, USA, 2008.
Slingo, J., Belcher, S., Scafie, A., McCarthy, M., Saulter, A., McBeath, K., Jenkins, A., Huntingford, C., Marsh, T., Hannaford, J., and Parry, S.: The Recent Storms and Floods in the UK, Report Met Office and CEH, Exeter, UK, 2014.

Teutschbein, C. and Seibert, J.: Regional climate models for hydrological impact studies at the catchment scale: a review of recent modelling strategies, Geogr. Compass, 4, 834–860, 2010.
Ushiyama, T., Sayama, T., Tatebe, Y., Fujioka, S., and Fukami, K.: Numerical simulation of 2010 Pakistan Flood in the Kabul river basin by using lagged ensemble rainfall forecasting, J. Hydrometeorol., 15, 193–211, doi:10.1175/JHM-D-13-011.1, 2014.
Wang, W., Bruyere, C., Duda, M., Dudhia, J., Gill, D., Lin, H. C., and Mandel, J.: ARW version 3 modeling system user's guide, Mesoscale & Miscroscale Meteorology Division, National Center for Atmospheric Research, available at: http://www.mmm.ucar.edu/wrf/users/docs/user_guide_V3/ARWUsersGuideV3.pdf (last access: 10 July 2014), 2010.
Ward, P. J., de Moel, H., and Aerts, J. C. J. H.: How are flood risk estimates affected by the choice of return-periods?, Nat. Hazards Earth Syst. Sci., 11, 3181–3195, doi:10.5194/nhess-11-3181-2011, 2011.
Xuan, Y., Cluckie, I. D., and Han, D.: Uncertainties in Application of NWP-Based QPF in Real-Time Flood Forecasting, Proc. of EU MITCH/FLOODRELIEF Symposium, Innovation, Advances and Implementation of Flood Forecasting Technology, Tromso, Norway, 2005.

HESSD
11, 7977–8011, 2014

Uncertainty propagation in a cascade modelling approach

J. P. Rodríguez-Rincón et al.

Table 1. Ensemble members defined for the multi-physics WRF ensemble.

Ensemble member	Micro-Physics	surface layer physics	Cumulus physics	Feedback/ sst_update
1	WSM5	5-Layer TDM	Kain–Fritsch Eta	off/on
2	WSM5	5-Layer TDM	Kain–Fritsch Eta	on/off
3	WSM5	5-Layer TDM	Kain–Fritsch Eta	on/on
4	WSM5	Noah	Kain–Fritsch Eta	off/off
5	WSM5	Noah	Kain–Fritsch Eta	off/on
6	WSM5	Noah	Kain–Fritsch Eta	on/on
7	Thompson	5-Layer TDM	Kain–Fritsch Eta	off/off
8	Thompson	5-Layer TDM	Kain–Fritsch Eta	off/on
9	Thompson	5-Layer TDM	Kain–Fritsch Eta	on/off
10	Thompson	5-Layer TDM	Kain–Fritsch Eta	on/on
11	Thompson	Noah	Kain–Fritsch Eta	off/off
12	Thompson	Noah	Kain–Fritsch Eta	off/on

HESSD
11, 7977–8011, 2014

Table 2. Error Metrics in the estimation of precipitation by members of the multi-physics ensemble (bold rows indicate the stations located within the Tonalá catchment).

Root-Mean Square Error (RMSE) and Normalised RMSE per Station considering Ensemble average													
Station No.	Multi-physics ensemble member												⟨Nor_RMSE⟩
	M1	M2	M3	M4	M5	M6	M7	M8	M9	M10	M11	M12	%
30167	**210.26**	**96.56**	**144.62**	**104.42**	**106.84**	**76.31**	**160.48**	**129.88**	**101.03**	**210.95**	**164.85**	**86.80**	**13.96**
27003	**544.34**	**578.19**	**564.46**	**474.81**	**427.30**	**516.95**	**458.25**	**484.05**	**568.20**	**572.30**	**385.17**	**479.47**	**35.13**
27007	**234.90**	**246.00**	**198.01**	**135.27**	**129.43**	**207.93**	**126.51**	**197.32**	**246.90**	**328.28**	**132.09**	**191.81**	**19.44**
27015	**96.68**	**129.89**	**151.02**	**194.33**	**235.76**	**179.69**	**152.06**	**152.60**	**118.97**	**116.87**	**260.49**	**188.20**	**24.01**
27074	173.37	211.87	191.22	197.46	78.94	148.88	174.92	247.65	187.98	207.39	123.09	157.21	17.19
27073	227.47	201.91	228.62	256.39	281.38	245.68	186.21	219.36	159.34	147.79	247.69	223.88	46.46
27075	**87.04**	**119.26**	**104.10**	**100.82**	**151.17**	**64.92**	**76.45**	**147.30**	**85.75**	**105.68**	**52.14**	**68.67**	**10.72**
27076	140.53	160.28	141.95	124.03	108.33	130.53	191.75	162.59	226.04	236.09	129.78	150.84	17.14
27077	89.10	113.42	83.60	225.48	252.24	207.73	254.20	282.40	110.77	83.93	203.01	192.86	30.57
27039	333.50	204.36	197.48	295.84	302.19	261.39	264.08	321.66	172.86	152.14	257.59	430.63	73.28
27054	123.18	30.77	45.28	113.16	119.18	77.41	106.84	112.68	118.83	127.43	110.06	106.67	34.75
27060	70.69	56.23	59.51	33.42	40.13	30.04	78.07	93.80	88.46	80.36	56.73	66.31	19.88
27024	160.33	137.81	140.76	120.58	127.54	73.57	148.27	136.47	145.12	167.79	153.26	151.87	85.04
27084	68.72	71.32	54.58	53.56	106.93	65.65	61.06	72.31	61.46	62.96	50.14	50.92	19.02
7365	172.91	117.44	103.02	252.03	139.79	163.49	301.52	216.38	179.67	129.71	271.88	210.11	24.52
27011	143.70	162.77	143.61	107.82	77.55	86.15	128.03	143.69	106.59	116.49	86.81	81.27	106.83
27036	81.46	60.69	27.36	61.69	19.14	35.64	23.58	45.89	22.13	40.23	39.22	55.55	12.04
27008	158.85	72.82	74.96	131.34	134.94	100.16	102.82	149.97	66.67	79.36	97.87	254.33	19.68
										Average {Rel_RMSE} catch.			**23.14**
										Average {Rel_RMSE} all			33.87

BIAS per Station and Ensemble Average													
Station No.	Multi-physics ensemble member												⟨BIAS⟩
	M1	M2	M3	M4	M5	M6	M7	M8	M9	M10	M11	M12	
30167	**0.71**	**0.90**	**0.81**	**1.07**	**1.12**	**0.99**	**0.80**	**0.85**	**0.91**	**0.71**	**1.23**	**1.06**	**0.93**
27003	**0.51**	**0.48**	**0.50**	**0.58**	**0.62**	**0.54**	**0.59**	**0.57**	**0.49**	**0.49**	**0.66**	**0.58**	**0.55**
27007	**0.72**	**0.71**	**0.79**	**0.91**	**0.91**	**0.78**	**1.13**	**1.26**	**0.73**	**0.61**	**0.90**	**0.80**	**0.85**
27015	**1.21**	**1.32**	**1.40**	**1.50**	**1.61**	**1.46**	**1.37**	**1.37**	**1.24**	**1.21**	**1.68**	**1.48**	**1.40**
27074	0.82	0.76	0.79	0.78	1.08	0.86	0.81	0.71	0.80	0.77	0.88	0.83	0.82
27073	1.74	1.65	1.74	1.83	1.91	1.80	1.58	1.70	1.47	1.44	1.80	1.72	1.70
27075	**0.92**	**0.85**	**0.88**	**0.88**	**1.20**	**0.96**	**0.90**	**0.80**	**0.89**	**0.86**	**0.98**	**0.93**	0.92
27076	0.86	0.82	0.86	0.91	0.95	0.89	0.79	0.84	0.73	0.71	0.89	0.85	0.84
27077	1.12	1.17	1.10	1.48	1.54	1.44	1.54	1.60	1.20	1.14	1.42	1.40	1.35
27039	2.41	1.87	1.84	2.26	2.29	2.11	2.13	2.36	1.73	1.64	2.09	2.84	2.13
27054	1.89	1.08	1.24	1.82	1.87	1.54	1.76	1.81	1.84	1.91	1.79	1.77	1.69
27060	1.42	1.33	0.72	1.08	1.20	1.05	1.47	1.57	1.54	1.49	1.32	1.39	1.30
27024	3.34	2.96	3.03	2.76	2.88	2.07	3.16	2.98	3.11	3.45	3.17	3.17	3.01
27084	1.32	1.35	1.17	1.23	1.61	0.78	1.27	1.36	1.27	1.29	1.07	1.01	1.23
7365	1.43	1.20	1.09	1.63	1.32	0.72	1.78	1.55	1.43	1.26	1.68	1.51	1.38
27011	3.57	3.91	3.55	2.93	2.33	2.49	3.33	3.58	2.91	3.09	2.56	2.45	3.06
27036	1.36	1.25	1.09	1.28	0.97	1.15	0.95	1.20	1.06	1.16	1.15	1.24	1.15
27008	1.37	1.07	1.05	1.29	1.31	1.20	1.21	1.35	0.99	0.93	1.19	1.62	1.22
										Average {Rel_RMSE} catch.			**0.94**
										Average {Rel_RMSE} all			1.42

HESSD
11, 7977–8011, 2014

Title Page
Abstract Introduction
Conclusions References
Tables Figures
◀I ▶I
◀ ▶
Back Close
Full Screen / Esc
Printer-friendly Version
Interactive Discussion

Table 2. Continuation of Table 2. Error Metrics in the estimation of precipitation by members of the multi-physics ensemble (blue rows indicate the stations located within the Tonalá catchment).

Nash-Sutcliffe Coefficient per Station and Ensemble average													
Station No.	Multi-physics ensemble member												⟨NSC⟩
	M1	M2	M3	M4	M5	M6	M7	M8	M9	M10	M11	M12	
30167	0.72	0.94	0.87	0.93	0.93	0.96	0.84	0.89	0.94	0.72	0.83	0.95	**0.88**
27003	0.16	0.05	0.09	0.36	0.48	0.24	0.40	0.33	0.08	0.07	0.58	0.34	**0.26**
27007	0.70	0.67	0.78	0.90	0.91	0.76	0.91	0.79	0.66	0.41	0.90	0.80	**0.77**
27015	0.88	0.78	0.70	0.50	0.27	0.57	0.70	0.69	0.81	0.82	0.11	0.53	**0.61**
27074	0.84	0.76	0.80	0.79	0.97	0.88	0.84	0.67	0.81	0.77	0.92	0.87	0.83
27073	−0.27	0.00	−0.28	−0.61	−0.94	−0.48	0.15	−0.18	0.38	0.46	−0.50	−0.23	−0.21
27075	**0.94**	**0.89**	**0.91**	**0.92**	**0.82**	**0.97**	**0.95**	**0.83**	**0.94**	**0.91**	**0.98**	**0.96**	**0.92**
27076	0.87	0.83	0.86	0.90	0.92	0.88	0.75	0.82	0.65	0.62	0.89	0.85	0.82
27077	0.82	0.70	0.84	−0.17	−0.46	0.01	−0.48	−0.83	0.72	0.84	0.05	0.15	0.18
27039	−4.41	−1.03	−0.90	−3.26	−3.44	−2.32	−2.39	−4.03	−0.45	−0.13	−2.23	−8.02	−2.72
27054	−0.46	0.91	0.80	−0.23	−0.36	0.42	−0.10	−0.22	−0.36	−0.56	−0.16	−0.09	−0.03
27060	0.60	0.75	0.72	0.91	0.87	0.93	0.51	0.29	0.37	0.48	0.74	0.65	0.65
27024	−7.99	−5.64	−5.93	−4.08	−4.69	−0.89	−6.68	−5.51	−6.36	−8.84	−7.21	−7.06	−5.91
27084	0.67	0.64	0.79	0.80	0.20	0.70	0.74	0.63	0.73	0.72	0.82	0.82	0.69
7365	0.50	0.77	0.82	−0.07	0.67	0.55	−0.54	0.21	0.45	0.72	−0.25	0.25	0.34
27011	−16.74	−21.76	−16.72	−8.99	−4.17	−5.38	−13.08	−16.74	−8.76	−10.66	−5.47	−4.67	−11.09
27036	0.61	0.78	0.96	0.78	0.98	0.93	0.97	0.88	0.97	0.91	0.91	0.82	0.87
27008	0.60	0.92	0.91	0.72	0.71	0.84	0.83	0.64	0.93	0.90	0.85	−0.03	0.73
										Average {Rel_RMSE} catch.			**0.63**
										Average {Rel_RMSE} all			−0.63

Correlation Coefficient per Station and Ensemble average													
Station No.	Multi-physics ensemble member												⟨Cor⟩
	M1	M2	M3	M4	M5	M6	M7	M8	M9	M10	M11	M12	
30167	**0.99**	**0.99**	**0.99**	**0.97**	**0.98**	**0.99**	**0.99**	**0.99**	**0.99**	**0.99**	**0.97**	**0.98**	**0.99**
27003	**0.95**	**0.96**	**0.97**	**0.97**	**0.98**	**0.98**	**0.99**	**0.99**	**0.99**	**0.99**	**0.99**	**0.99**	**0.98**
27007	**0.98**	**0.97**	**0.97**	**0.97**	**0.97**	**0.97**	**0.97**	**0.97**	**0.97**	**0.95**	**0.98**	**0.97**	**0.97**
27015	**0.97**	**0.96**	**0.97**	**0.94**	**0.93**	**0.95**	**0.95**	**0.95**	**0.94**	**0.94**	**0.93**	**0.94**	**0.95**
27074	0.98	0.98	0.98	0.98	0.99	0.98	0.99	0.98	0.98	0.98	0.99	0.99	0.98
27073	0.95	0.96	0.95	0.94	0.94	0.94	0.92	0.92	0.91	0.92	0.94	0.94	0.94
27075	0.98	0.98	0.98	0.98	0.99	0.99	0.99	0.99	0.99	0.99	0.99	0.99	**0.99**
27076	0.98	0.98	0.97	0.97	0.97	0.97	0.97	0.97	0.96	0.96	0.97	0.97	0.97
27077	0.96	0.95	0.96	0.96	0.95	0.96	0.95	0.95	0.97	0.97	0.95	0.96	0.96
27039	0.95	0.95	0.94	0.93	0.94	0.94	0.94	0.94	0.95	0.95	0.94	0.93	0.94
27054	0.91	0.96	0.94	0.93	0.93	0.94	0.91	0.92	0.91	0.90	0.93	0.93	0.93
27060	0.96	0.97	0.97	0.96	0.97	0.97	0.95	0.95	0.96	0.96	0.97	0.96	0.96
27024	0.91	0.93	0.92	0.90	0.91	0.95	0.89	0.90	0.89	0.89	0.94	0.94	0.91
27084	0.91	0.91	0.92	0.94	0.92	0.95	0.92	0.91	0.92	0.92	0.93	0.93	0.92
7365	0.93	0.93	0.94	0.92	0.94	0.97	0.91	0.92	0.91	0.92	0.91	0.92	0.93
27011	0.94	0.94	0.95	0.93	0.95	0.96	0.89	0.93	0.91	0.92	0.91	0.91	0.93
27036	0.99	0.99	0.99	0.99	0.99	0.99	0.99	0.99	0.99	0.99	0.99	0.99	0.99
27008	0.97	0.96	0.96	0.96	0.96	0.96	0.96	0.96	0.97	0.96	0.96	0.96	0.96
										Average {Rel_RMSE} catch.			**0.97**
										Average {Rel_RMSE} all			0.95

Table 3. Error metrics in the estimation of river discharge by the rainfall–runoff model using the 12 members of the multi-physics ensemble.

	Error metrics per ensemble member and ensemble average for the hydrological model												
	M1	M2	M3	M4	M5	M6	M7	M8	M9	M10	M11	M12	⟨Ens Av⟩
RMSE ($m^3 s^{-1}$)	163.05	122.49	110.53	230.13	201.49	153.81	147.25	131.42	123.96	127.51	232.76	131.68	156.34
NSC	0.84	0.91	0.93	0.69	0.76	0.86	0.87	0.90	0.91	0.90	0.68	0.90	0.84
Cor	0.97	0.98	0.98	0.97	0.95	0.96	0.95	0.96	0.96	0.96	0.94	0.95	0.96
BIAS	0.83	0.89	0.92	1.29	1.20	0.86	1.08	0.90	0.94	0.94	1.24	1.05	1.01
NRMSE (%)	39.75	29.86	26.95	56.11	49.12	37.50	35.90	32.04	30.22	31.09	56.75	32.11	38.12

HESSD
11, 7977–8011, 2014

Uncertainty propagation in a cascade modelling approach

J. P. Rodríguez-Rincón et al.

HESSD
11, 7977–8011, 2014

Uncertainty propagation in a cascade modelling approach

J. P. Rodríguez-Rincón et al.

Table 4. Error metrics in the estimation of river discharge by the hydrodynamic model using the 12 members of the multi-physics ensemble.

Error metrics	Comparison of flooded areas between numerical results from running ensemble members vs. Observed: Ensemble Member												⟨Ensemble average⟩
	M1	M2	M3	M4	M5	M6	M7	M8	M9	M10	M11	M12	
BIAS	0.872	0.893	0.904	0.917	0.910	0.872	0.940	1.006	1.022	1.073	1.040	1.119	0.964
FAR: False Alarm Ratio	0.132	0.143	0.148	0.154	0.149	0.132	0.562	0.817	0.824	0.847	0.865	0.877	0.453
POD: Probability of Detection	0.757	0.765	0.770	0.776	0.750	0.757	0.782	0.817	0.824	0.847	0.856	0.877	0.799
POFD:Probability of False Detection	0.107	0.119	0.125	0.132	0.112	0.107	0.145	0.176	0.185	0.210	0.205	0.225	0.154
CSI: Critical Succes Index	0.868	0.857	0.852	0.846	0.851	0.868	0.834	0.812	0.806	0.790	0.791	0.784	0.831
True Skill Statistics	0.650	0.646	0.645	0.644	0.653	0.650	0.645	0.641	0.639	0.637	0.641	0.652	0.645

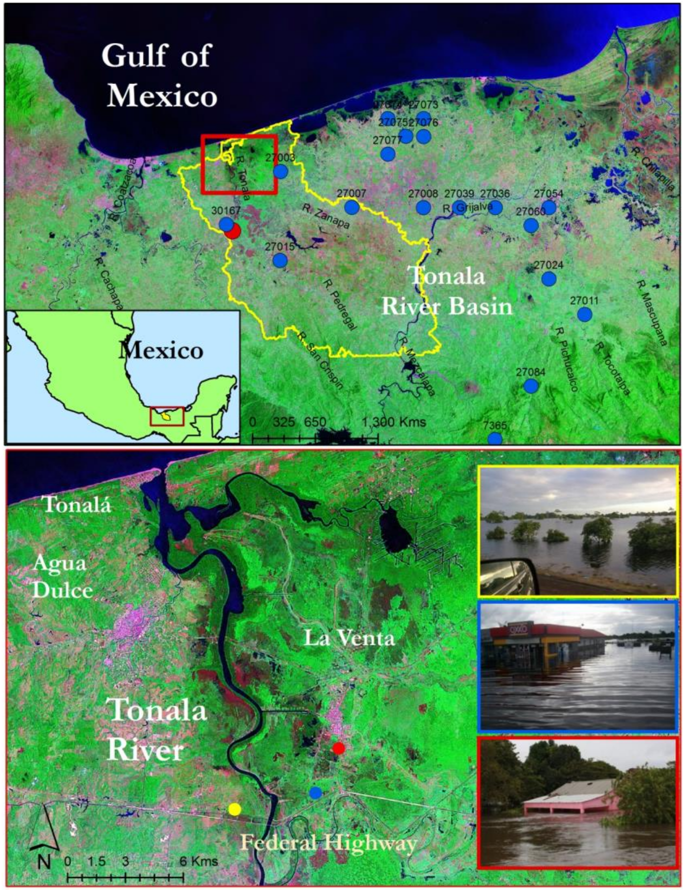

Figure 1. Top panel: location of the Tonala River basin in Mexico, blue line represents the boundary limits of the catchment; blue dots illustrate the location of weather stations; red dot: streamflow gauge. Bottom panel: zoom of the study area and photographs of observed impacts; yellow, blue and red dots represent the location at which photos were taken.

HESSD
11, 7977–8011, 2014

Uncertainty propagation in a cascade modelling approach

J. P. Rodríguez-Rincón et al.

Title Page
Abstract Introduction
Conclusions References
Tables Figures
◂ ▸
Back Close
Full Screen / Esc
Printer-friendly Version
Interactive Discussion

Figure 2. Numerical setup of the WRF with a nested domain covering Mexico. Domain 1: 25 km resolution; Domain 2: 4 km resolution; the orange region illustrates the Tonalá catchment.

HESSD
11, 7977–8011, 2014

Uncertainty propagation in a cascade modelling approach

J. P. Rodríguez-Rincón et al.

Title Page
Abstract Introduction
Conclusions References
Tables Figures
◀| |▶
◀ ▶
Back Close
Full Screen / Esc
Printer-friendly Version
Interactive Discussion

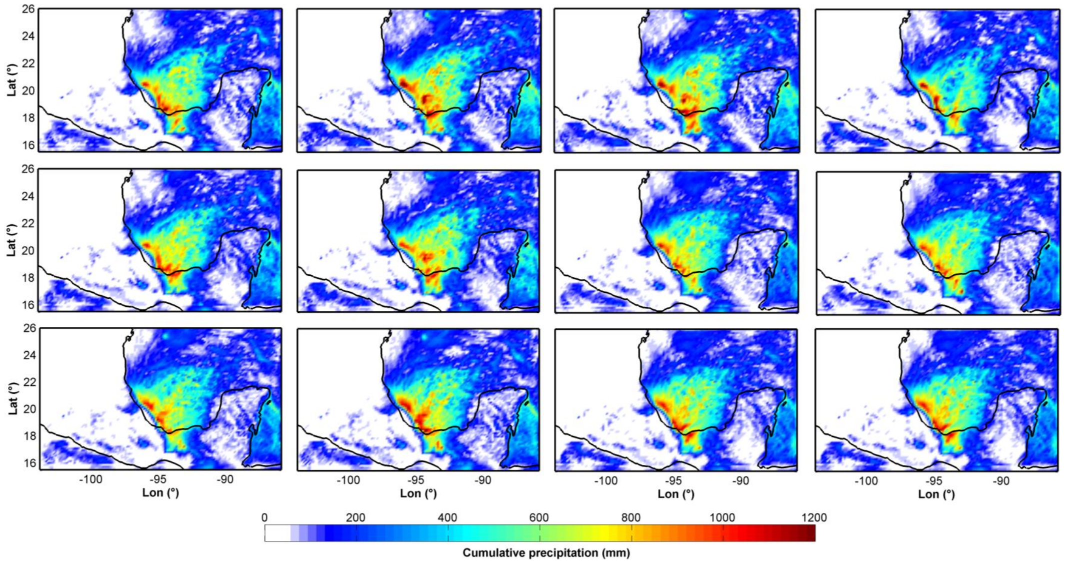

Figure 3. Cumulative precipitation fields estimated by the WRF model using the 12 members of the multi-physics ensemble (27 October 2009–12 November 2009).

HESSD
11, 7977–8011, 2014

Uncertainty propagation in a cascade modelling approach

J. P. Rodríguez-Rincón et al.

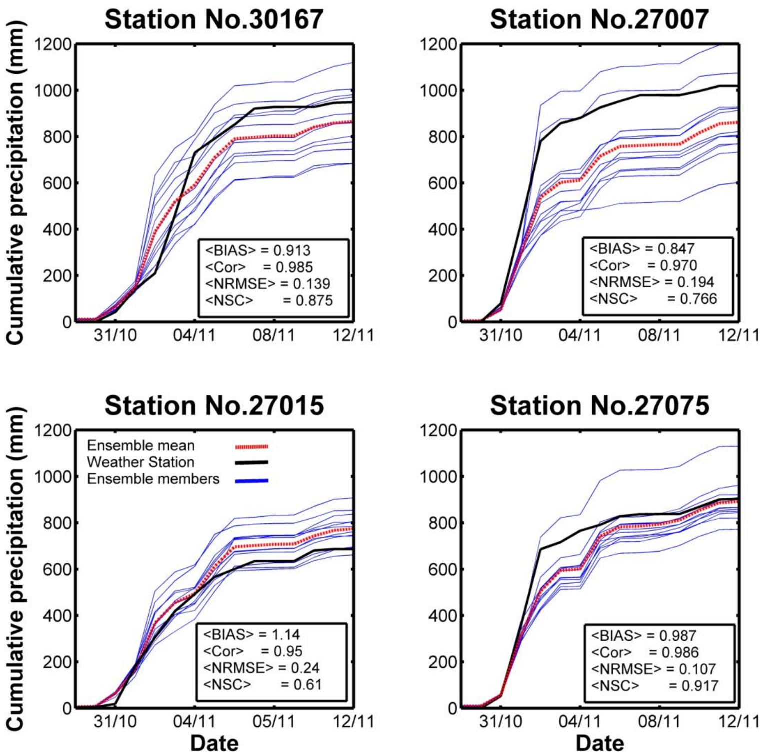

Figure 4. Comparison of cumulative precipitation estimated by the 12 members of the WRF model (blue lines) and its mean (red line) vs. measurements (black solid line) at four weather stations from 27 October 2009 to 12 November 2009.

HESSD
11, 7977–8011, 2014

HESSD
11, 7977–8011, 2014

Uncertainty propagation in a cascade modelling approach

J. P. Rodríguez-Rincón et al.

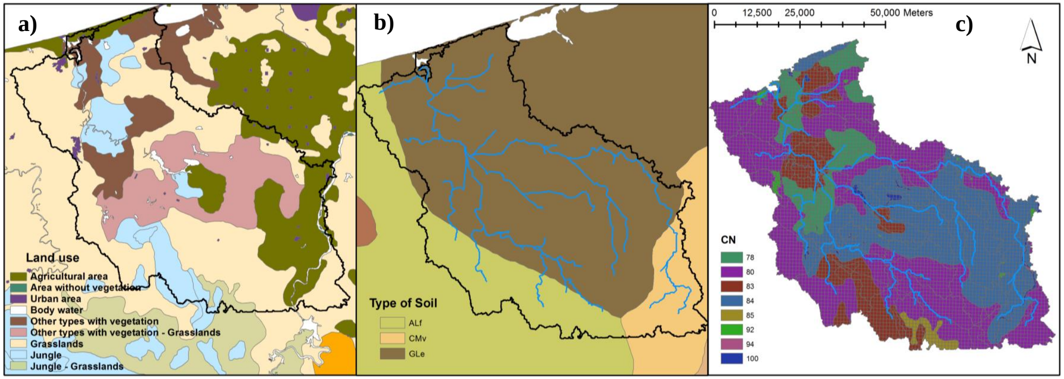

Figure 5. Input data parameters in the hydrological model; **(a)** land use; **(b)** pedology; **(c)** river network, curve number and grid.

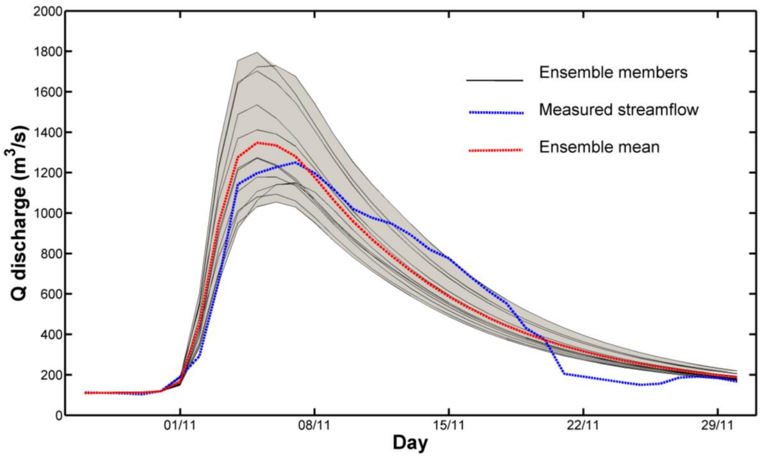

Figure 6. Calculated hydrographs using the rainfall–runoff model with WRF ensemble precipitation fields as input data; grey shaded area illustrates the uncertainty bounds (maximum and minimum); the red line shows the measured river discharge for this event.

HESSD
11, 7977–8011, 2014

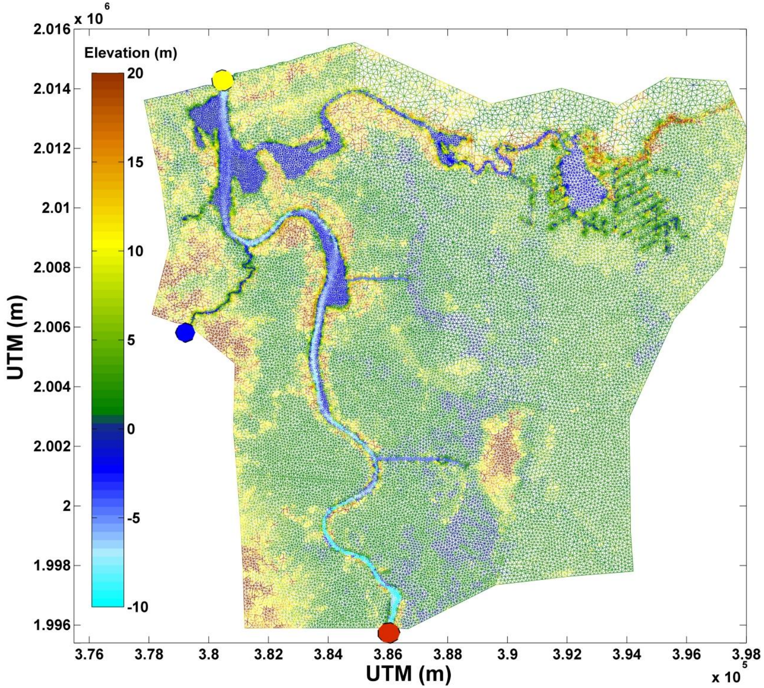

Figure 7. Model domain along with the numerical mesh and elevation data in the study area; Boundary conditions are represented by blue dot: Agua Dulcita river; red dot: input hydrograph; yellow dot: river-mouth.

HESSD
11, 7977–8011, 2014

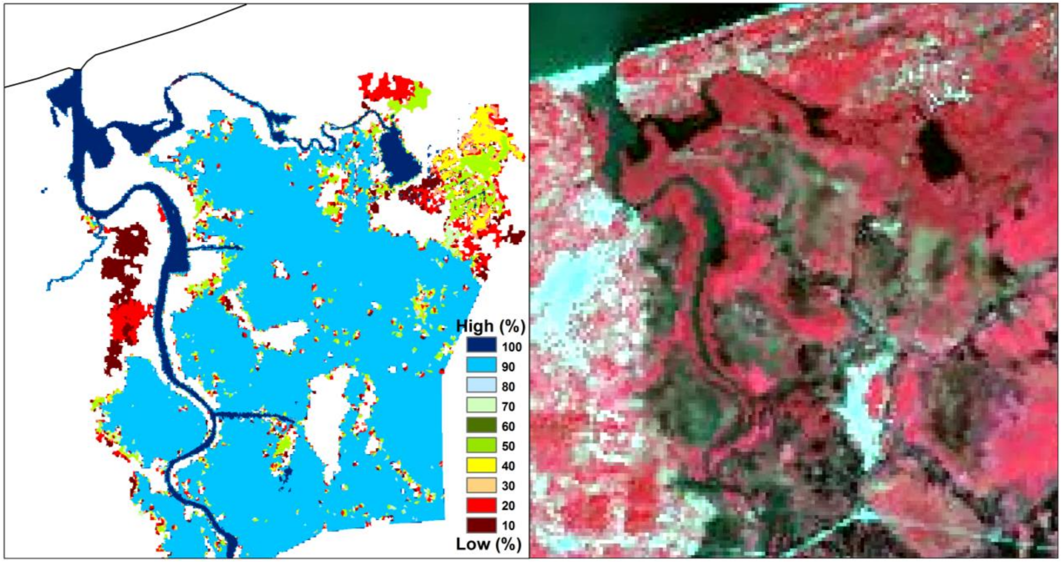

Figure 8. Data vs. model comparison of flood extent; probabilistic flood map derived from ensemble runs with the hydrodynamic model (left panel); infrared SPOT image corresponding to the 15 November 2009 (right panel).

HESSD
11, 7977–8011, 2014

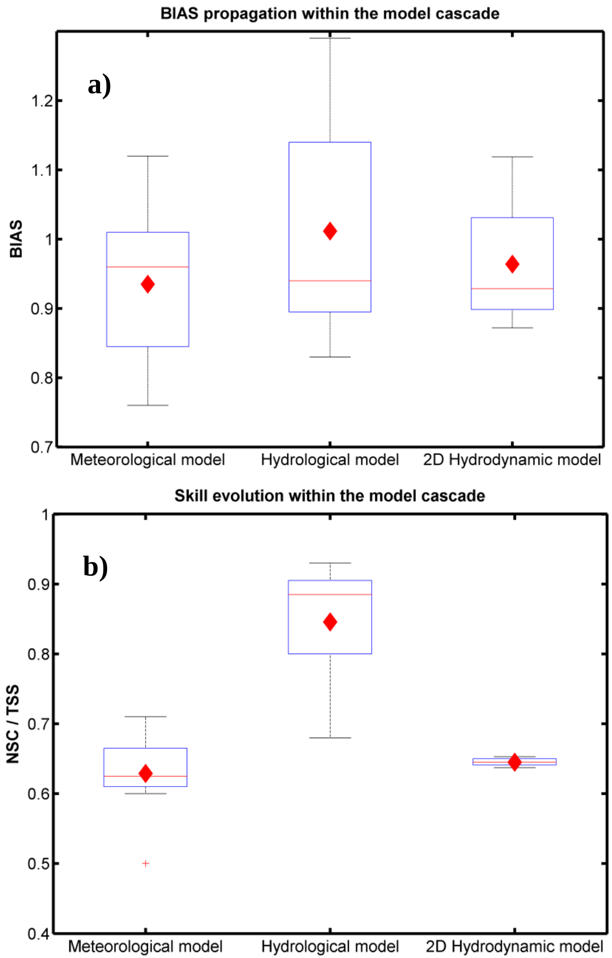

Figure 9. (a) BIAS and **(b)** skill propagation within the model cascade (meteorological–hydrological–hydrodynamic); diamonds: corresponding ensemble mean value.

HESSD
11, 7977–8011, 2014

Uncertainty propagation in a cascade modelling approach

J. P. Rodríguez-Rincón et al.

Title Page
Abstract Introduction
Conclusions References
Tables Figures
◀I ▶I
◀ ▶
Back Close
Full Screen / Esc
Printer-friendly Version
Interactive Discussion